CFD Analysis of Turbulent Flows In Hydroelectric Plant Intakes Application to ASFM Technology

L. Bouhadji, D.D. Lemon, D. Topham, D. Billenness and D. Fissel
ASL Environmental Sciences Inc.
Sidney, British Columbia, Canada

Abstract

Turbulent flows in the Lower Monumental powerhouse intake are investigated using computational fluid dynamics. Simulations are carried out with a $k - \varepsilon$ turbulence model. The performance of the CFD model is examined by comparing the mean flow and turbulence statistics with the Acoustic Scintillation Flow Meter technique developed by the company. The CFD results show a good agreement with the ASFM data.

Introduction

ASL has developed a non-intrusive Acoustic Scintillation Flow Meter (ASFM) for monitoring velocities and total flows in the intakes of low head hydroelectric plants. These measurements allow hydro engineers to evaluate turbine operation efficiency and changes due to turbine performance and/or use of fish protection devices within the intake. The basic operation of the ASFM system can be found in the paper by Lemon, Billenness and Lampa (2002).

To address the operational requirements, accuracies approaching 1 % in the total flow measurements are being sought. Several factors may affect the flow accuracy of the ASFM. These factors are:

- Positioning of the transducer arrays in the intake and the number of transducer units.
- Blockage and deflection of the flow by one or more cylindrical cross members supporting the frames on which the acoustic transducers are mounted.
- Effect of the top, bottom and side wall boundary layers.
- Upstream effects: obstructions, obstacles (the trash rack or fishscreens).
- Turning of the flow at the intake.

To gain an understanding into the importance of some of these factors and in order to optimize the accuracy of the Acoustic Scintillation Flow Meter technique, numerical studies using CFD (Computational Fluid Dynamics) have been undertaken. All the simulations were performed on the University of Victoria's supercomputing facility (Minerva). Two and three-dimensional detailed simulations have been made to investigate a number of complex geometric configurations and flow parameters in the Lower Monumental plant intake. Only 2D results will be presented in this paper. Preliminary results with a $k - \varepsilon$ turbulence model, have been compared to available ASFM data and show a very good agreement. The presence of the trash rack is shown to be an important factor in the alteration of the mean velocity and turbulent kinetic energy over a significant downstream distance in the intake. The influence of these effects on the accuracy of the ASFM flow measurements is discussed in this paper.

Numerical implementation

The numerical simulations, including the mesh generation, are performed using the commercial code CFX 4.3 from AEA Technologies Ltd. This code uses a multi-block finite-volume method to solve the discretized Navier-Stokes equations in conjunction with various turbulence models. The code also provides a pre-processor for grid-generation. In the finite volume method, the governing differential equations are integrated over control volumes defined by the grid. The diffusive and advective fluxes and the source terms in the volume integrals are then discretized using various techniques. The discretization method must be carefully selected to ensure both adequate accuracy and numerical stability. CFX provides several numerical schemes. Based on the physics of the flow (incompressible, turbulent, complex geometry), experience pointed to two higher order schemes: MUSCL (Monotonic Upwind Scheme for Conservative Laws) and the CCCT scheme which is a modification of the QUICK (Quadratic Upwind Interpolation for Convective Kinematics) which is bounded and eliminates numerical overshoots. The MUSCL scheme is a high-order upwind scheme (second order accurate for advection), which however has reduced accuracy due to its dissipative truncation error. The CCCT scheme is third order accurate for the advective terms and is accordingly less dissipative than the MUSCL scheme and may result in improved accuracy. The two different numerical schemes were used in conjunction with a grid refinement study. Simulation results were compared in terms of resolution of expected physical features associated with the complex geometries including inlet curvature, flow obstacles, bypass slots, trash racks and steps. While both schemes performed adequately, CCCT provided better resolution in wake regions and was accordingly used for all simulations performed thereafter.

Turbulence modelling

Resolution of the instantaneous fluctuating flowfield in turbulent flows is not feasible for complex flows. Engineering methods implemented in CFD rely on the numerical solution of the Reynolds-averaged Navier-Stokes (RANS) equations in conjunction with turbulence models of varying degrees of complexity, ranging from algebraic eddy viscosity to Reynolds stress models. In the eddy viscosity models, as the basic $k-\varepsilon$ or $k-\varepsilon$ with renormalization group (RNG) models, the Reynolds stresses are linearly related to the mean velocity gradients in a similar way as in the relationship between the stress and strain tensors in laminar Newtonian flows. In Reynolds stress turbulence models (RSM), the eddy viscosity hypothesis is not invoked. Instead, a transport equation is defined for each component of the Reynolds stress tensor. This model provides a conceptually more correct representation of turbulence characteristics such as anisotropy and the effect of extra strains, but is more complex and computationally intensive. As a result of the substantially lower computational effort required, the $k-\varepsilon$ model is still one of the most commonly used turbulence models for the solution of practical engineering flows. There is, however, a large amount of evidence that though the $k-\varepsilon$ model reproduces qualitatively many of the important flow features, it is not totally satisfactory in some complex flow situations, particularly these involving flow separation. In this work, in addition to the $k-\varepsilon$, the RNG $k-\varepsilon$ model has been also tested. This variant includes a strain dependent correction that has been shown to improve the predictive capabilities of the model. All the simulations carried out in this project, have been done with both models and no significant difference in the results, has been found. The RNG $k-\varepsilon$ model results, although available, are not presented in this paper.

Computational domains and boundary conditions

The computational domain of the 2D Lower Monumental intake is shown on Figure 1-a. The model domain encompasses one of the three intake bays. Two cases are treated; the first without the trash rack in place and the second with it in place. The boundary conditions and the transducer unit positions are also shown in the same figure. The main slope of the floor is equal to 1/6 (Slope A). The inlet of the domain is placed 35 m upstream. Symmetry conditions are specified at a small distance from the "normal low pool" level (137.78') and at the top of the slot. All solid walls are treated using the logarithmic law of the wall assuming smooth surfaces. The diameter of the top and bottom frame cylinders are, respectively, 8.625" and 10.75". 322,156 grid nodes and 199 blocks are used when the trash rack is removed. When it is present, 1,101,376 grid points and 1249 blocks are used. In both cases three different inlet velocities were tested. All were constant, uniform profiles equal to U_0=0.4214, 0.616 and 0.769 m/s, giving volume flow rates of Q_1=113.28, Q_2=165.58 and Q_3=206.72 m^3/s. Some of the flowfield results have been compared to the ASFM data collected in Unit 6 (see table 1).

Unit	Bay A	Bay B	Bay C	Conditions
6	175.349	200.875	206.79 •	Off Cam, screens out
6	179.248	205.199 •	212.619	//
6	188.523•	216.857	225.107	//
6	141.862	162.148	167.278•	//
6	144.822	165.148•	169.83	//
6	166.375•	190.435	196.77	//
6	106.855	120.119•	124.129•	//
6	113.948•	129.243	132.831	//
6	99.964 •	113.409•	117.327•	On Cam, screens out

Table 1: Flow rates computed from the ASFM data (m^3/s). The dot highlights the cases compared to the CFD results.

Results

Figure 1-b shows the grid distribution upstream and within the two dimensional intake. A close up is shown around the intake entrance when the trash rack is present (Fig. 1-c). There are six trash rack panels placed one on another up to the top of the intake entrance. As a result, five thicker horizontal beams are present. The minimum grid size Δx (next to the wall) is $\sim$ 5 mm, the maximum is equal to 1.57 m and is located at the outlet, while $\Delta y_{max} \sim 0.7$ m at a middle position, in the intake.

Figures 2-(a,b) show the mean streamwise velocity distribution $\bar{U}$ and mean turbulent kinetic energy distribution $\bar{k}$ upstream and within the intake for $Q_1 = 113.28\, m^3/s$. The physics of the flow for the other two velocities stays basically the same and the introduction of non-dimensional variables, normalized by the inlet velocity U_0, is therefore a better approach to analyse the data.

Without the trash rack in place, a separated flow takes place at the top entrance of the intake over a distance $\Delta x \sim 3.5$ m and behind the gate slot over a distance $\Delta x \sim 2$ m. The flow accelerates from $\bar{U}$=1.8 to 2.6xU_0 between x=9 and 40 m. The velocity reaches a maximum of $\sim$ 4.65xU_0 above and below the bottom cylinder at $\sim$ 1/3rd radius distance. High turbulent intensity levels are found in recirculation zones. The flow accelerates when increasing the inlet velocity and when going downstream (convergent flow). The turbulent kinetic energy increases, in the recirculation zone, as well. At the floor, the thickness of the boundary layer is found equal to 25 cm at x=20.9 m, and basically, does not change for the three different flow rates. $\bar{k}$ reaches a maximum value in the boundary layer. Behind the cylinder, a maximum deficit is found and is about a diameter wide. $\bar{k}$ has enhanced values within 2 ft above the floor. The flow acceleration increases this value and a maximum is reached at $\sim$1.3 ft.

The presence of the trash rack clearly disturbs the flow even far downstream (Fig. 2-(c,d)). The presence of the horizontal beams is found to decrease the velocity at the top of the intake entrance and increase it towards the floor (see fig. 2-(a,b) for comparison). $\bar{k}$ is also increased in the entire downstream section. Figure 3 shows a comparison of the velocity vector and the speed magnitude distribution with and without the trash rack present, at the top entrance of the intake. The flow coming down to the intake, from the top upstream part of the domain, is slowed down by the first beams. In the middle and bottom sectors, the approach flow is progressively horizontal and is therefore more accelerated past the trash rack.

Figures 4 shows the profiles of the velocity component $\bar{U}$ and the turbulent kinetic energy, at the ASFM plane of measurements (x=22.37 m), for the three different flow rates tested. A comparison is made when the trash rack is present (TRI) and when it is removed (TRO) on the same plot. The effect of the trash rack is immediately noticed. The $\bar{U}$ component magnitude is reduced at the top section of the profile and accelerated at the lower part, when the trash rack is present and this confirms the observations made earlier, on figure 2. The signature of the thick beams is still visible at a distance x=22.37 m ($\sim$ 73.4 ft) downstream. Four major velocity deficits caused by the first thick beams from the floor, are clearly present at this distance and become more significant when the inlet bulk velocity is higher. The fifth large beam is too close to the ceiling and its deficit is not propagated at the plane of measurement. At this plane, the maximum deficits from the other 4 beams are 0.115, 0.07, 0.05 and 0.03xU_0 at y=3.7, 6.8, 9.5 and 11.6 m. These deficits are 2.2, 1.9, 1.6 and 1.6 m wide, respectively. Two other small deficits (0.7 m wide) are also visible at y=1.5 and 2.3 m. They belong to the wakes of the first beams close to the bottom. Due to the relatively high acceleration in this region and in between beams, these wakes have been directed and propagated downstream and have not diffused and merged at this distance. Note that the thickness of the boundary layer increases from 25 cm to $\sim$ 50 cm at x=20.9 m, when the trash rack is present.

Figure 4-b, shows the corresponding mean kinetic energy profiles. High values of $\bar{k}$ are found, with or without trash rack at the bottom, up to 0.7 m from the floor and at the top, up to 1.4 m from the roof. $\bar{k}$ increases with the acceleration of the flow, as well. The maximum turbulent intensity value is found $\sim$ 14% higher, when the trash rack is present, for all the flow rates (the turbulent intensity is computed as $I_t = 2\bar{k}/U_0^2$). At the top, I_t is equal to 0.85 and 0.73, respectively, when the trash rack is present and when it is removed (16% difference). In the middle section of the profile, the turbulent intensity is in the range $0.035 < I_t < 0.045$. When the trash rack is removed, this value is negligable.

Comparison CFD-ASFM data

The two dimensional CFD results are compared to the available ASFM data, collected at the Lower Monumental plant intake in January 2002. The ASFM data were measured in two different units: Unit 2 and Unit 6. Each unit includes three bays: Bay A, Bay B and Bay C. For each individual bay, ASFM measurements were made at a total of 20 acoustic paths. The numerical results are compared to the closest ASFM flow rates.

Figure 5 shows the mean streamwise velocity component profiles at the plane of measurements. A comparison is made when the trash rack is present (black solid line) and removed (black dashed line). The numerical simulations have been carried out for three different flow rates: Q=113.283, 165.58 and 206.72 m^3/s and the ASFM data have been collected at Unit 6. Note, however, that the ASFM flow rates are not exactly the same as the ones of the simulations. The figures on the left side correspond to the dimensional profiles. The profiles on the right side are normalized by the inlet velocity.

The two dimensional numerical results show a good agreement with the ASFM measurements for all tested flow rates.
When the trash rack is present, the flow is reduced in the middle and top sections of the profile and accelerates in the bottom part, the velocity deficits from the beams are propagated downstream and the comparison shows a better match with the ASFM data. The predicted cylinder wake width (bottom frame) is, however, smaller than the measured one. This is probably due to the presence of a rope wrapped spirally around the cylinder, which has not been taken into account in the simulations. By increasing the total cylinder diameter from 10.75" to 11.25", this rope would certainly increase the thickness of the wake.
The comparison shows that the number of transducers units should be increased to fully resolve the deficits and accelerations arising from the trash rack, downstream at the plane of measurements. Up to ten more transducers would be required. Normalizing the variables by a characteristic velocity allows comparison of the CFD results with the ASFM measurements in each of the 3 intake bays. Since the simulations have been done on the same bay, with the same inlet conditions (with a different magnitude, though), the normalized CFD results show no change in the shape of the profiles for the three different inlet bulk velocity tested and the numerical results become very close to the ASFM data. The normalized ASFM profiles (see fig. 6), however, show differences among discharges in the same bay. This is likely due to differences in inlet conditions when the measurements were made.

Conclusion

The simulations have demonstrated the strong influence of the trash racks in the alteration of the downstream freestream flow features and the floor boundary layer characteristics within the intake. Some of the conclusions drawn from this study are listed below:

- A two dimensional study, though with a removed trash rack, has shown reasonable agreement with the ASFM data.

- More accurate and realistic numerical results have been obtained by incorporating the entire 2D trash rack at the intake entrance. The good agreement obtained with the ASFM measurements demonstrates that the three dimensional effects played by the side wall boundary layers might be low on the spanwise average quantities. The trash rack has been found to increase the velocity flow field in the bottom region of the intake and to slow it down at the top region. The velocity deficit, caused by the thick horizontal beams (8 in wide), propagates as far downstream as the plane of ASFM measurements ($\sim$ 73 ft). Their effects are emphasized, when the upstream flow field is more accelerated. Indeed, even, thinner beams (4 in wide), located near the floor, where the acceleration is found higher, have some effects on the velocity deficit at the plane of measurements. This can be explained by the fact that, the wakes generated by these beams have less opportunity to diffuse when strong acceleration is present in between the structures.

- A three-dimensional computation without trash rack (not presented in this paper), has shown that the 3D effects (due to the side walls) are concentrated in a region close to the gate slot and close to the bottom frame ($\sim 2\,to\,2.4\,m$ below the first transducer and up to 1.5 m above the floor). In the remaining domain (along, almost, the entire plane of measurements), the side wall boundary layer thickness does not change significantly. Note that the boundary layer increases with the presence of the trash rack.

- These results demonstrate that it is feasible to model both the velocity and turbulent kinetic energy distribution in a large hydroelectric plant. The results of the simulations can be used to optimize the placement of ASFM sampling paths. Extending the simulations to three dimensions, including the trash rack, is presently underway. It is expected that the results will allow the effects of the distribution of turbulence and velocity in the intake on the accuracy of the ASFM measurements to be estimated.

References

D.D. Lemon, D. Billenness and J. Lampa, *Recent advances in Estimating Uncertainties in Discharge Measurements with the ASFM,* Proceedings of the Hydro 2002 (Development, Management Performance) Conference, Kiris, Turkey, November, 2002. Published by International Journal of Hydropower & Dams, Aqua-Media Intl., Sutton, Surrey, U.K.

Authors

Latif Bouhadji, Ph.D., graduated in Fluid Mechanics from the Fluid Mechanics Institute of Toulouse, France, in 1998. He was a research associate at the University of Victoria's CFD Laboratory before joining ASL in 2002. He is a CFD modeler at ASL Environmental Sciences.

David D. Lemon, M.Sc., graduated in Oceanography from the University of British Columbia, Vancouver, in 1975 and worked for ASL since 1978. He has worked extensively on the application of underwater acoustics to measuring flow, and has been responsible for the development of the ASFM. He is currently the President of ASL, with responsibility for Research and Development.

David Billenness, M.A.Sc., graduated in Mechanical Engineering from the University of Victoria, British Columbia, in 1995 and worked for ASL since 1997. He currently heads the field flow measurements program associated with the ASFM.

David Topham, Ph.D., graduated in aeronautical engineering in 1959, from Loughborough College, U.K., and obtained his Ph.D. in 1970 in the field of high circuit voltage interruption. In 1973, he joined the Federal Govt. of Canada working on Arctic related environmental problems of oil and gas exploration. He is currently working with ASL on the ASFM development.

David Fissel, M.Sc., graduated in Oceanography from the University of British Columbia, Vancouver, in 1975. He was a founding partner in ASL Environmental Sciences Inc. and is the founding President and CEO of ASL AQFlow Inc.

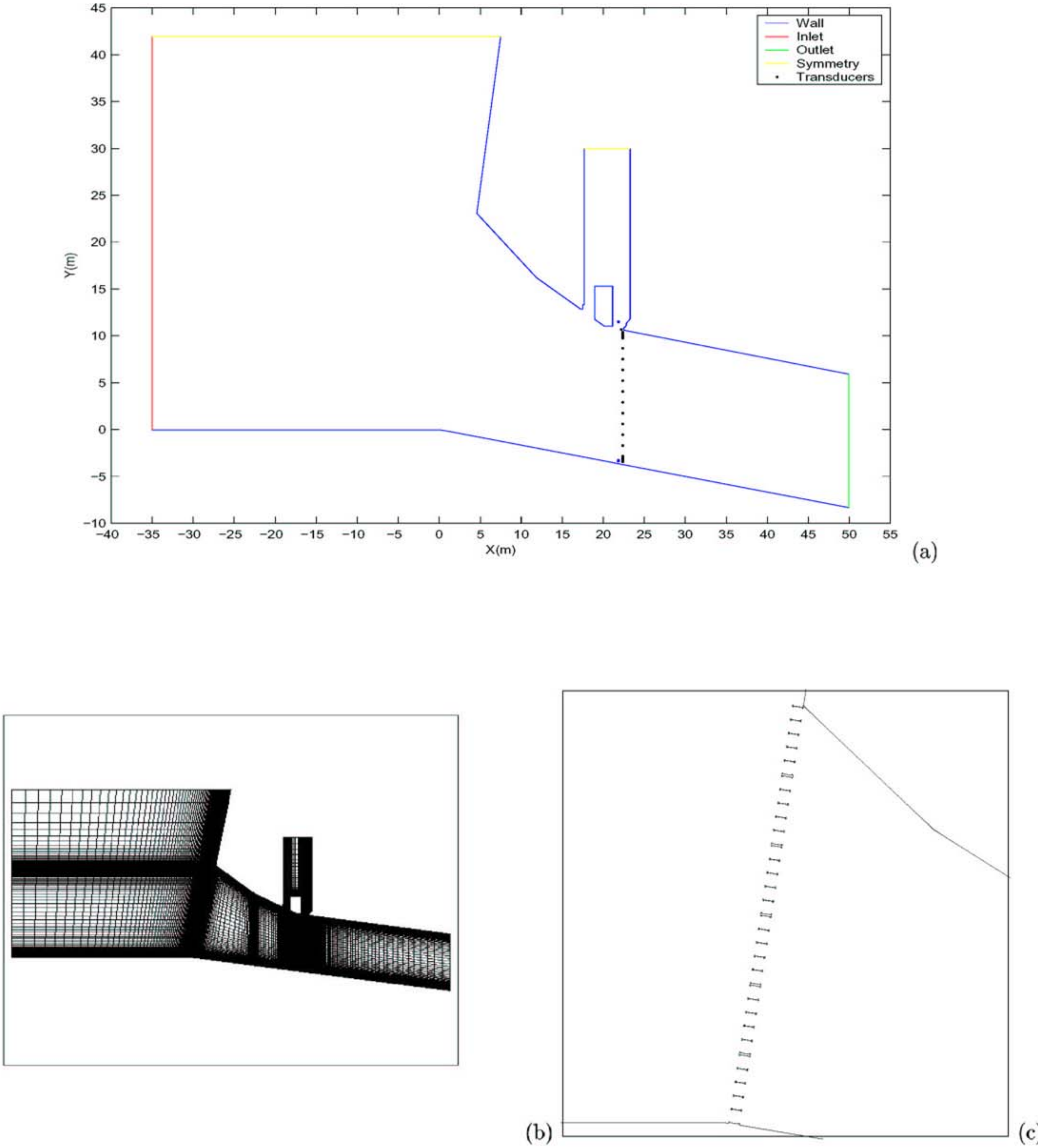

Figure 1: a,b)-Computational domain and the 2D mesh of the Lower Monumental intake with no trash rack. The transducers placement and the boundary conditions are illustrated. c)- Location of the 2D trash rack at the intake entrance.

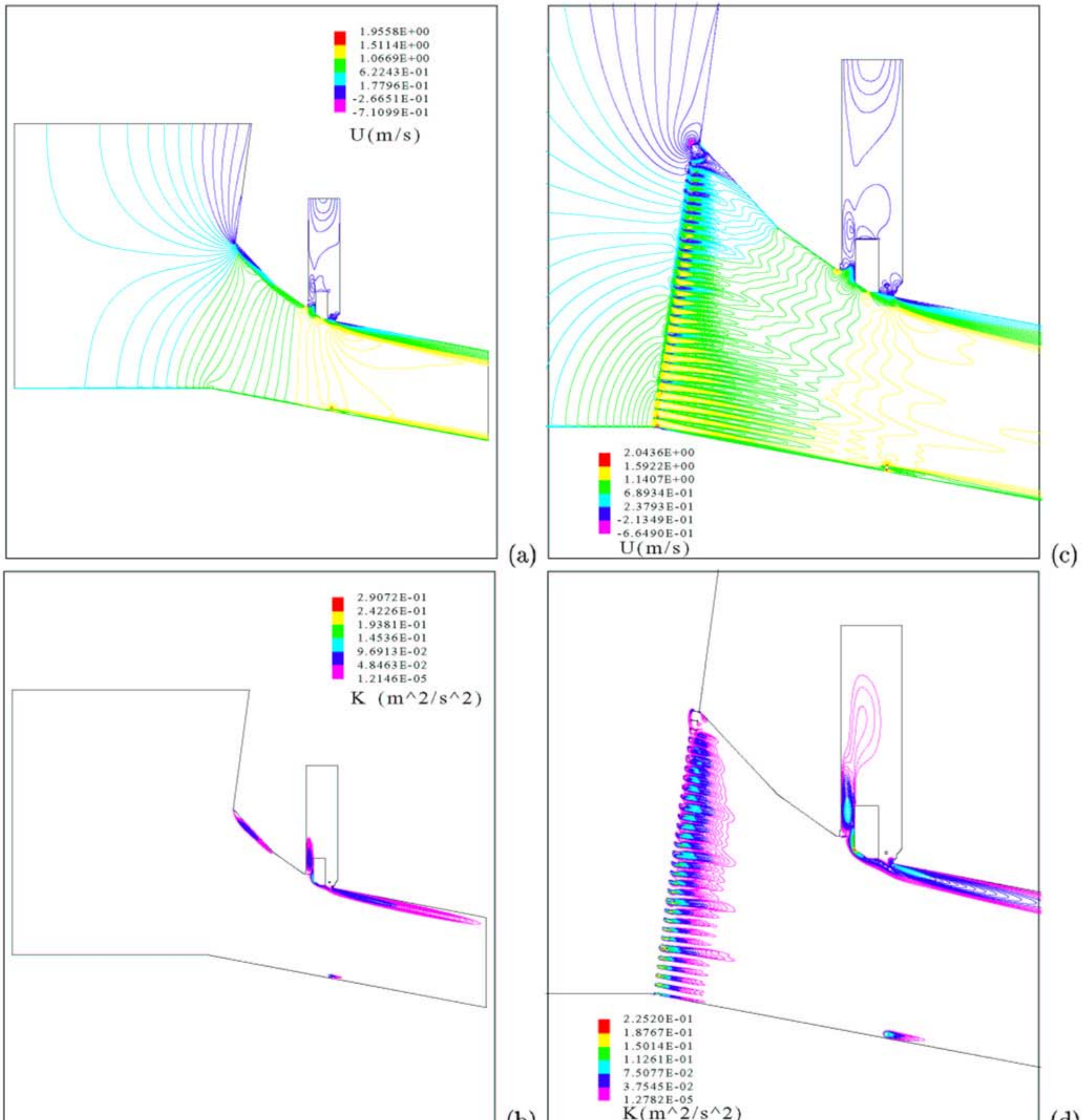

Figure 2: a,b)-Mean streamwise velocity and turbulent kinetic energy distribution in the Lower Monumental Intake. Trash rack and screens out. Q=113.283 m^3/s. c,d)- Same distribution with the trash rack present. Q=113.283 m^3/s.

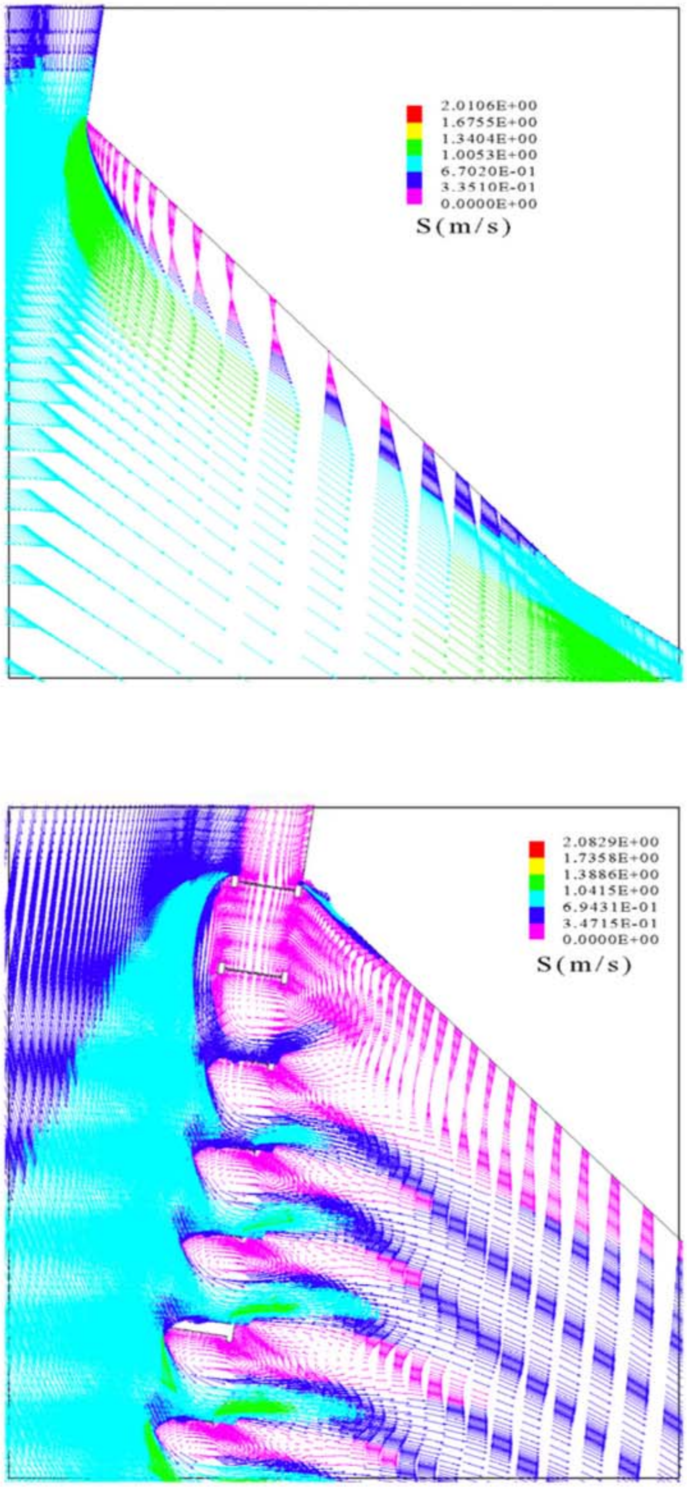

Figure 3: Close up at the top entrance of the intake showing the speed magnitude and velocity vector distribution for Q=113.283. a)-The trash rack is removed. b)-The trash rack is present.

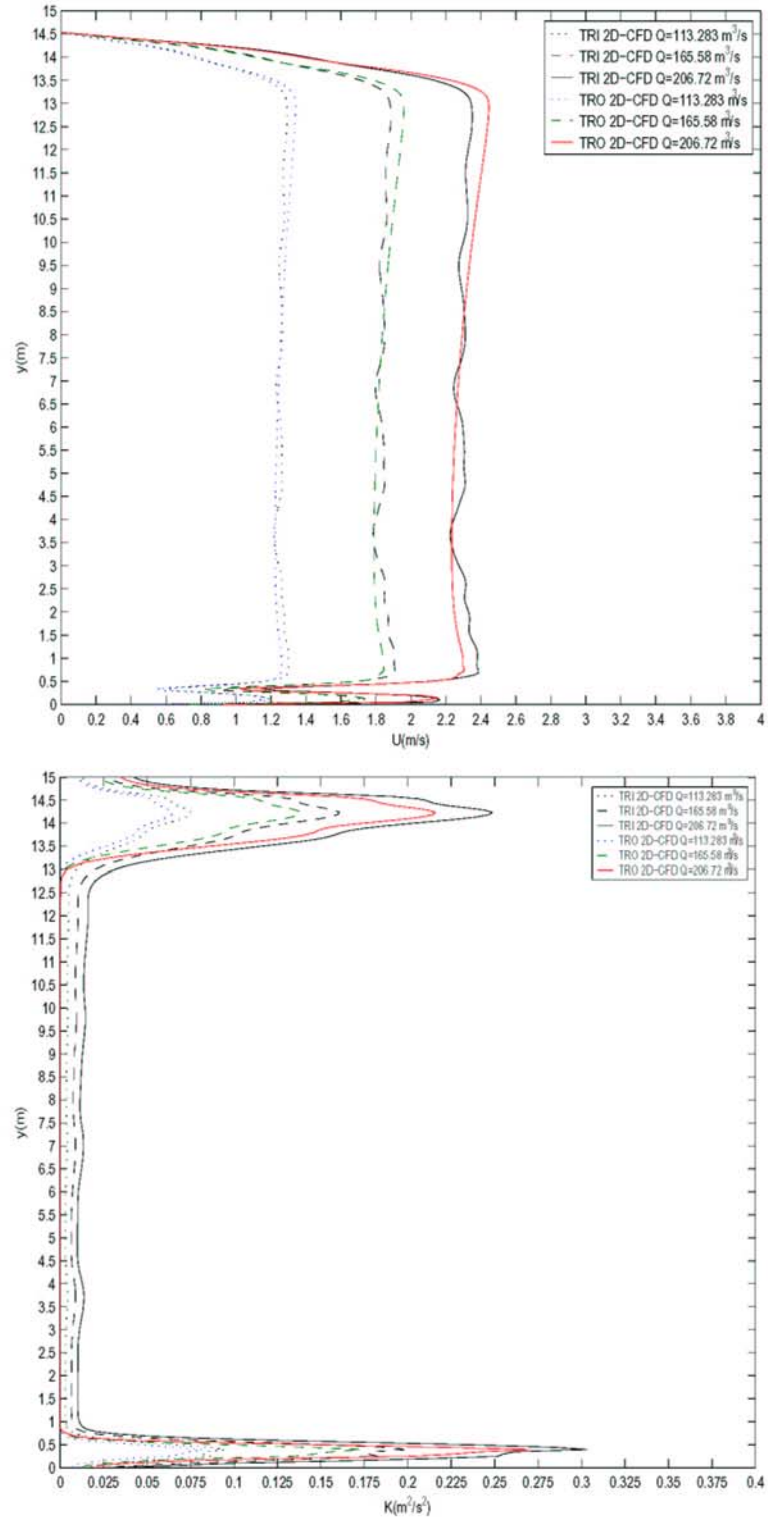

(a)

(b)

Figure 4: U velocity and Turbulent kinetic energy profiles at the plane of measurement. Comparison is made when the trash rack is present (TRI) and when it is removed (TRO) at three different flow rates. Q=113.283, 165.58 and 206.72 m^3/s.

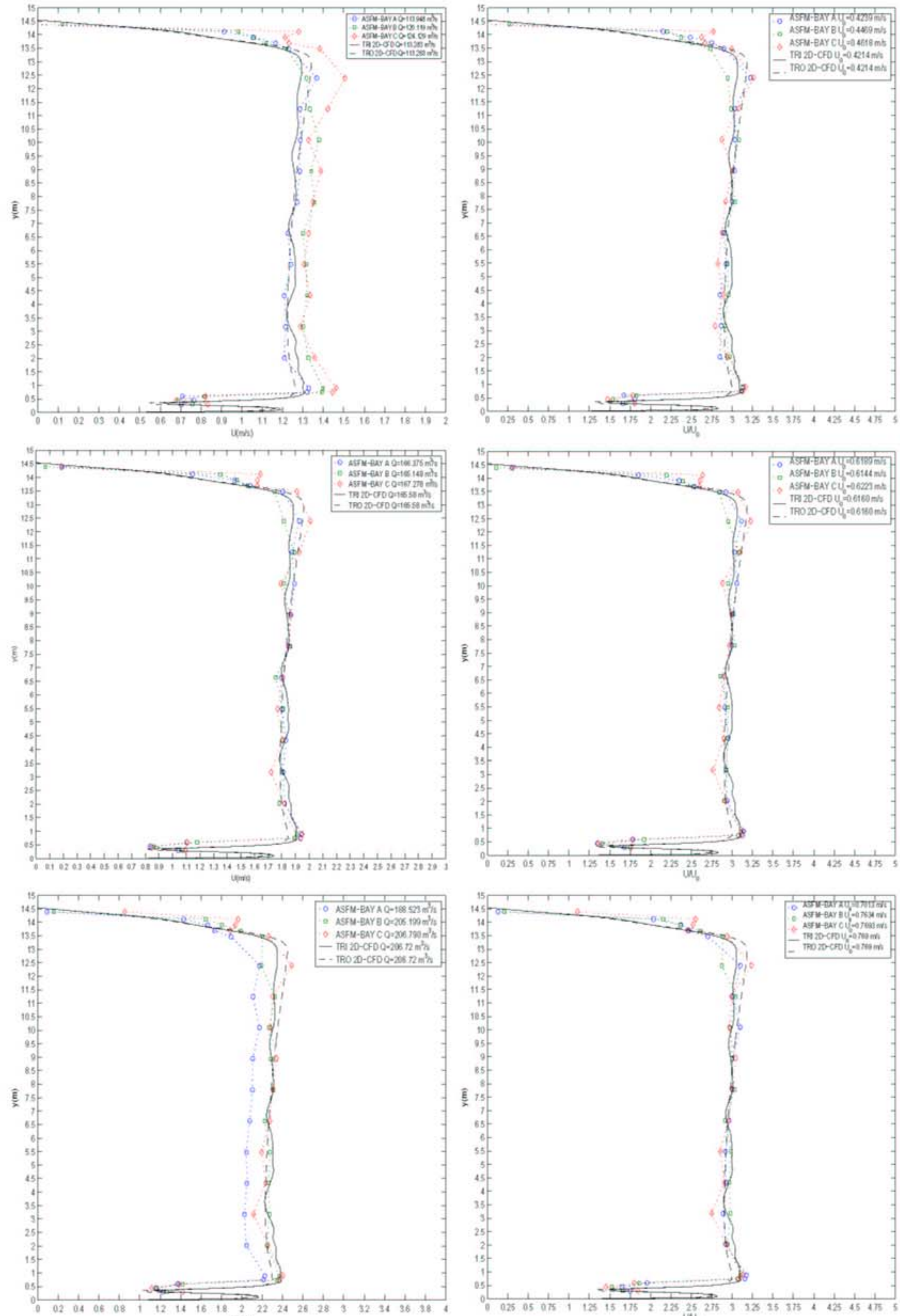

Figure 5: Mean streamwise velocity profiles at the plane of measurement. A comparison is made when the trash rack is present (TRI) and removed (TRO). a,d)-Q=113.283 m^3/s; b,e)-Q=165.58 m^3/s; c,f)-Q=206.72 m^3/s. The ASFM data are from Unit 6. The figures on the left side denote the dimensional profiles. In the right side column, the profiles are normalized by the inlet velocity U_0.

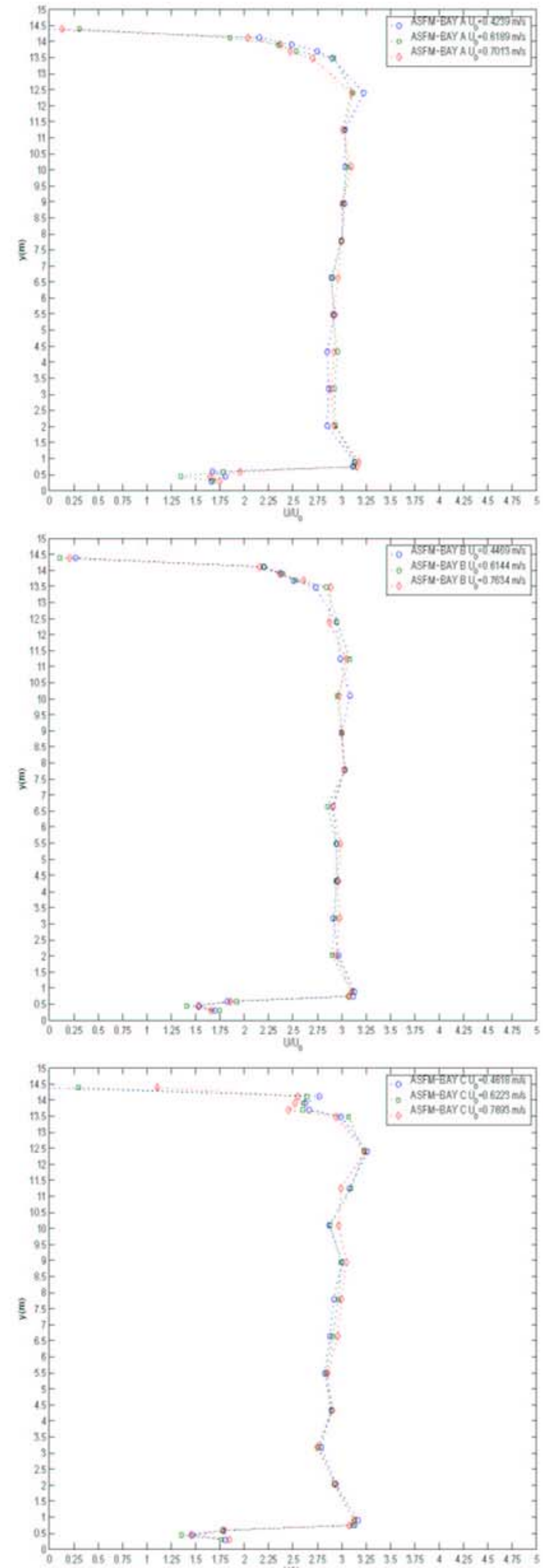

Figure 6: ASFM mean streamwise velocity profiles at the plane of measurement normalized by the inlet velocity U_0, at three different bays.